ELSEVIER

First-order reversal curve (FORC) diagrams for pseudo-single-domain magnetites at high temperature

Adrian R. Muxworthy *, David J. Dunlop

Geophysics, Physics Department, University of Toronto, Toronto, ON, Canada

Abstract

The recently developed first-order reversal curve (FORC) technique for rapidly examining magnetic domain state has great potential for paleomagnetic and environmental magnetic investigations. However, there are still some gaps in the basic understanding of FORC diagrams, in particular the behavior of pseudo-single-domain (PSD) grains and the contribution of magnetostatic interactions. In this paper we address some of these problems. We report the first FORC diagrams measurements on narrowly sized and well-characterized synthetic PSD through multidomain (MD) magnetite samples. The FORC diagrams evolve with grain size from single-domain (SD)-like to MD-like through the PSD grain size range. Since each sample contains grains of essentially a single size, individual PSD grains evidently contain contributions from both SD-like and MD-like magnetic moments, in proportions that vary with grain size; the evolving FORC diagrams cannot be due to physical mixtures of SD and MD grains of widely different sizes. The FORC diagrams were all asymmetric. Small PSD samples have FORC diagrams with a distinctive closed-contour structure. The distributions of the larger MD grains display no peak, and lie closer to the interaction-field axis. To assess the effect of magnetostatic interactions, we measured FORC diagrams between room temperature and the Curie temperature. On heating the FORC distributions contract without changing shape until $\sim 500°$C. Above this temperature the diagrams become more MD-like, and in addition become more symmetric. The temperature dependence of the interaction-field parameter is proportional to that of the saturation magnetization, in accordance with Néel's interpretation of the Preisach diagram. The decrease in asymmetry with heating suggests that the origin of the asymmetry lies in magnetostatic interactions. The magnetic hysteresis parameters as a function of temperature were determined from the FORC curves. As the grain size decreased the normalized coercive force was found to decrease more rapidly with temperature.
© 2002 Elsevier Science B.V. All rights reserved.

Keywords: magnetite; magnetic domains; coercivity; reversals

1. Introduction

The composition and grain-size distribution of magnetic minerals determine the overall magnetic properties of a rock or sediment and the stability of its natural remanent magnetization through geological time. With the increasing interest in using natural magnetic mineral assemblages in en-

* Corresponding author. Present address: Department of Geology and Geophysics, University of Edinburgh, King's Buildings, West Mains Road, Edinburgh EH9 3JW, UK. Fax: +44-131-668-3184.
  E-mail address: adrian.muxworthy@ed.ac.uk
(A.R. Muxworthy).

vironmental and paleoclimatic studies, it is becoming essential to have magnetic methods that characterize both composition and grain size of the magnetic minerals. Conventional methods, calibrated using well-defined synthetic samples, are unfortunately sometimes ambiguous in characterizing natural rocks and sediments [1].

The smallest magnetic grains, containing only a single domain (SD), have the strongest and most stable remanence. The iron oxide minerals, e.g. magnetite (Fe_3O_4) and maghemite (γ-Fe_2O_3), dominate the magnetic properties of sediments and most continental rocks, both because of their common occurrence and their strong spontaneous magnetization. Grains above the SD/multidomain (MD) threshold size (70–100 nm; [2]) are often termed pseudo-single-domain (PSD) because their remanence is also relatively strong and stable. PSD grains are usually volumetrically dominant in a typical rock or sediment.

It is essential to have a reliable method or methods of determining the domain state in geological samples. In absolute paleointensity studies, SD grains produce the most reliable results and larger MD grains the least meaningful results, with PSD grains intermediate in their reliability [3]. Paleoclimatic information is often revealed by subtle changes in grain-size distribution, as revealed by domain state, while the same grain-size variations complicate the determination of relative paleofield intensity from the same sediments [4]. One standard way of determining the domain state is measurement of magnetic hysteresis. Hysteresis parameters, such as coercive force H_C, remanent coercive force H_{CR}, saturation magnetization M_S and the saturation remanence M_{RS}, are often used for this purpose, either individually or in combination as in the plot of Day et al. [5]. However, the Day plot is non-unique: various combinations of mineral composition, grain size, internal stress and magnetostatic grain interactions can produce the same set of hysteresis parameters [6,7].

2. The first-order reversal curve (FORC) diagram

Roberts et al. [1] and Pike et al. [8–10] have developed a new method of mineral and domain state discrimination using FORCs. Constructing a FORC diagram requires lengthy measurements and intricate mathematical analysis which have only recently become possible with fast and sensitive vibrating-sample magnetometers (VSMs) and alternating-gradient magnetometers. The FORC diagram is constructed from a set of partial hysteresis curves (FORCs or first-order return branches: [11,12]). Each FORC is measured by saturating the sample, decreasing the field to a value H_a, and reversing the field sweep to the saturated state in a series of field steps (H_b). This process is repeated for many values of H_a. The magnetization $M(H_a, H_b)$ measured at each step generates the FORC distribution [1]:

$$\rho(H_a, H_b) \equiv -\partial^2 M(H_a, H_b) / \partial H_a \partial H_b \qquad (1)$$

When the FORC distribution is plotted as a contour plot of $\rho(H_a, H_b)$, it is convenient to rotate axes by changing coordinates from $\{H_a, H_b\}$ to $\{H_C = (H_b - H_a)/2, \ H_U = (H_b + H_a)/2\}$.

The FORC method originated in the phenomenological Preisach–Néel theory of hysteresis. In the analogous Preisach [13] diagram (with $a = H_a > 0$, $b = H_b < 0$), Néel [14] showed that for interacting SD grains, H_C corresponds to the coercive force H_C of each SD loop in the absence of interactions and that H_U is the local interaction field. It follows that $\rho(H_a, H_b)$ is the product of two independent distributions, the coercivity distribution $g(H_C)$ and the interaction-field distribution $f(H_U)$. The Preisach and FORC distributions are equivalent in some situations, but in general the FORC diagram is less restrictive. For example, the FORC diagram does not assume a symmetric distribution. This symmetry restriction has been addressed in Preisach theory by the moving Preisach model, in which H_U changes in proportion to the overall magnetization of the sample. This modification has been moderately successful (e.g. [15]), but introduces some ambiguity into the interpretation of measured Preisach diagrams.

In general the philosophy of the FORC method is to reject any underlying model-dependent assumptions or approximations, e.g. as in the phenomenological Preisach model. Instead the FORC

distribution is simply a well-defined mathematical transformation of a suite of experimentally measured partial hysteresis curves [1].

Our study presents measurements of FORC distributions for PSD grains of magnetite at high temperature approaching the Curie temperature. FORC distributions for sized PSD magnetites have not been reported previously, although Preisach diagrams have been [15–19]. Another objective of the present study was to test whether or not profiles through the FORC distribution parallel to the H_C and H_U axes have the properties expected of distributions of coercivities $g(H_C)$ and interaction fields $f(H_U)$ as suggested by Néel's interpretation of Preisach theory. Dunlop and West [16] and Dunlop et al. [19] determined Preisach diagrams using forward and reverse remanence measurements as a function of temperature. Their most striking finding was that the parameter H_U usually interpreted as the interaction field did not vary with temperature T as $M_S(T)$ as expected for magnetostatic interactions, but in fact as the coercive force $H_C(T)$. We carry out the same test on profiles of our FORC distributions and find a temperature variation of $f(H_U)$ that is compatible with $M_S(T)$.

3. Sample description

Two sets of PSD and MD samples of different origin are studied in this paper. The first set, W(0.3 μm), W(1.7 μm), W(7 μm) and W(11 μm), consists of commercial magnetites from Wright Industries produced six months before the experiments and stored in a desiccator. Grain sizes determined from scanning electron micrographs were all log-normally distributed. X-ray diffraction (XRD) spectra measured shortly after receiving the samples appeared to be those of pure magnetite, within experimental error. Six months later at the time the FORC measurements were made at the Institute for Rock Magnetism, Minnesota, USA, Mössbauer spectra measured using a ^{57}Co source revealed oxidation parameters z ranging from 0.088 for W(0.3 μm) to 0.009 for W(11 μm). It is uncertain whether partial oxidation occurred during the six months of storage or whether the samples were initially non-stoichiometric.

The stoichiometry was magnetically estimated from Curie and Verwey temperatures. A typical high-field thermomagnetic curve measured with a Princeton Measurements VSM is shown in Fig. 1. The Curie temperatures of 583 ± 1°C for the four samples are slightly higher than the 575–580°C of stoichiometric magnetite [20], again indicating a degree of non-stoichiometry. Verwey transitions determined from low-temperature susceptibility measurements using a Lakeshore Cryotronics AC susceptometer were sharp in the larger grains, indicating stoichiometric magnetite, but broader in the smaller grains.

The second set of samples, H(7.5 μm), H(39 μm) and H(76 μm), was produced by hydrothermal recrystallization [21]. The magnetic properties of these samples have been described in detail by Muxworthy and McClelland [22] and Muxworthy

Table 1
Grain-size distributions and room-temperature hysteresis data for the studied samples

Sample name	Mean (μm)	SD (μm)	Mean AR	$\mu_0 H_C$ (mT)	$\mu_0 H_{CR}$ (mT)	M_{RS}/M_S
W(0.3μm)	0.3	0.2	1.4	33.7	54.5	0.281
W(1.7 μm)	1.7	0.2	1.4	16.1	39.1	0.149
W(7 μm)	7	3	1.0	6.2	24.9	0.065
W(11 μm)	11	3	1.8	4.6	20.4	0.044
H(7.5 μm)	7.5	3.0	–	2.2	18.5	0.016
H(39 μm)	39	9	–	1.1	24.2	0.007
H(76 μm)	76	25	–	0.9	26.7	0.005

The grain-size distributions were determined from scanning electron micrographs. The aspect ratio (AR) is the ratio of the long axis over the short axis. No aspect ratio was measured for the hydrothermally produced samples as they were nearly all symmetrical.
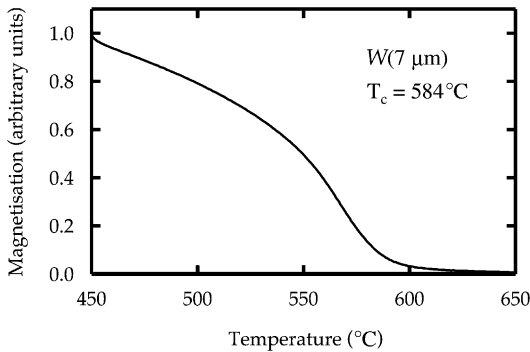
Fig. 1. High-temperature detail of a thermomagnetic curve for sample W(7 μm). The Curie temperature is 584°C. This value is a little above the value often quoted for stoichiometric magnetite (575–580°C, [20]). The applied field was 1 T.

[23]. Mean grain sizes and standard deviations are summarized in Table 1. XRD and Mössbauer spectra indicated pure magnetite and the samples had been stored for several years in non-oxidizing environments. However, to check for possible oxidation, warming curves for a saturation isothermal remanence induced at 35 K were measured using a Quantum Designs SQUID magnetometer. A sharp Verwey transition was observed, indicating stoichiometric magnetite and that little or no oxidation had occurred in these samples.

Magnetic hysteresis parameters measured at room temperature for all seven samples using the VSM are summarized in Table 1 and shown with the mixing model of Dunlop [6] in the form of a Day plot in Fig. 2. The hydrothermally grown samples have very low values of H_C and M_{RS}/M_S, close to those reported previously [22], indicating low dislocation densities in agreement with previous studies [24]. The Wright samples have higher H_C and M_{RS}/M_S values than the hydrothermal samples of similar size, indicating a higher level of internal stress related either to the method of preparation or non-stoichiometry. H_C and M_{RS}/M_S values decrease as grain size increases in agreement with other studies [5–7,25]. In Fig. 2, the smallest sample W(0.3 μm) plots within the PSD region indicated by Dunlop [6]. The other Wright samples lie just above this PSD region, and the hydrothermal samples plot in the MD region.

4. Experimental methods

FORCs were measured using the VSM described above, for all seven samples at room temperature and at high temperature up to ≈ 600°C for the Wright samples. The samples were dispersed in high-temperature cement and heated in a helium atmosphere which, if anything, is slightly reducing (J. Marvin, personal communication, 2002). As there was a problem with the absolute temperature calibration for the VSM when measuring the FORCs, the VSM was initially manually calibrated for a range of temperatures using a second thermocouple. FORC diagrams were then measured for these set temperatures. Uncertainty in the absolute temperature at any step was ± 5°C. However, during the actual measurements at a particular step, the temperature did not vary by more than ± 1°C.

The technique used for fitting the FORC surface was identical to that outlined by Roberts et al. [1], where a full description is given. Briefly, to evaluate the FORC distribution $\rho(H_a,H_b)$ (Eq. 1) at a point P, a local square grid of points is considered with P at the center. The number of points on the local grid depends on a smoothing
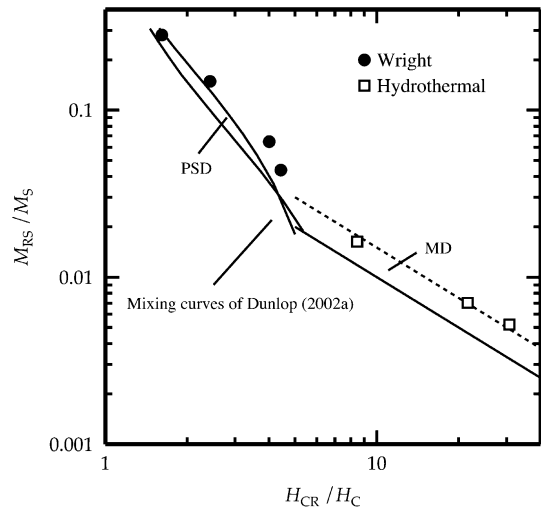

Fig. 2. M_{RS}/M_S versus H_{CR}/H_C (Day plot) for the four Wright samples and the three hydrothermally grown magnetite samples. Also depicted are PSD and MD regions determined by Dunlop [6]. The hysteresis parameters were measured at room temperature.
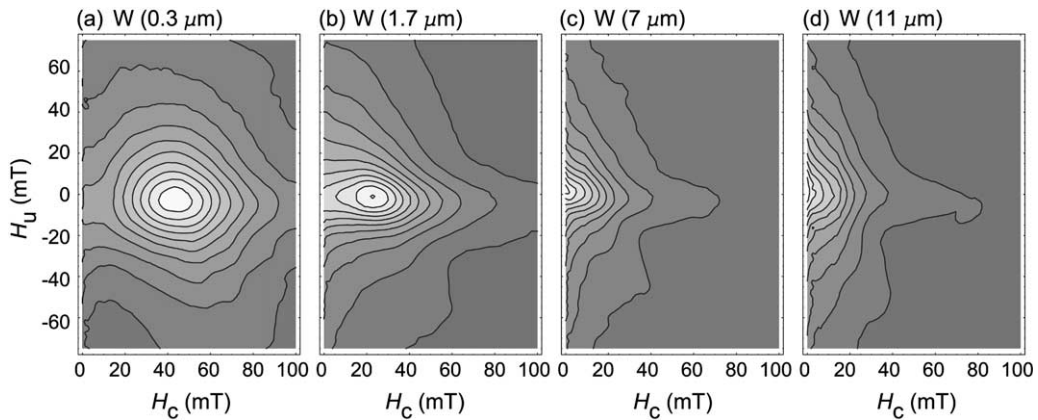
Fig. 3. Room-temperature FORC diagrams for the four Wright samples. Scaling factors: (a) SF = 2, (b) SF = 3, (c) SF = 2 and (d) SF = 2.

factor (SF) and is given by $(2SF+1)^2$. For example for SF = 3, the smoothing is performed across a 7×7 array of data points. The magnetization at these points is then fitted with a polynomial surface of the form: $a_1 + a_2 H_a + a_3 H_a^2 + a_4 H_b + a_5 H_b^2 + a_6 H_a H_b$, where the value $-a_6$ represents $\rho(H_a, H_b)$ at P. Taking the second derivative in Eq. 1 magnifies the noise that is inevitably present in the magnetization measurements. Therefore, FORC diagrams produced with SF = 1 contains greater noise. This can be reduced by increasing the size of SF; however, the cost of increasing SF is that fine scale features disappear. In addition, in calculating the FORC distribution, no points are determined in the region between the H_U axis and $2 \times SF \times FS$ (FS = field spacing during the FORC measurement) and it is necessary to make an extrapolation of the FORC surface onto the H_U axis. Increasing SF increases the error in this extrapolation.

The FORC distribution of an assemblage of non-interacting SD particles is narrowly confined to the central horizontal axis [1,8]. Magnetostatic interactions between SD grains causes vertical spread of the contours about the peak, while thermal relaxation of fine SD particles shifts the FORC distribution to lower coercivities [8,9]. In contrast MD FORC distributions have no central peak, and the contours tend to spread broadly parallel to the $H_U = 0$ axis [1,10].

5. Room-temperature results on PSD and MD magnetite

Room-temperature FORC diagrams are shown for the four Wright samples in Fig. 3, and for the three hydrothermally grown samples in Fig. 4. The FORC distributions change markedly with grain size. Samples W(0.3 μm) and W(1.7 μm) display distinct closed-contour peaks between 25 and 50 mT in the FORC distribution, while the peak of the FORC distribution lie near the origin for the larger samples. The cross-section of the FORC distribution along the H_C axis is plotted in Fig. 5. According to the Preisach–Néel theory, this plot is the coercivity distribution $g(H_C)$. This distribution is seen to evolve continuously with grain size (Figs. 3–5). The hydrothermally grown samples (Fig. 4) display more MD-like FORC diagrams than the Wright samples (Fig. 3) for samples with similar grain sizes, e.g. W(7 μm) and H(7.5 μm). This reflects differences in internal stress and dislocation densities.

Profiles of the FORC distributions in the H_U direction gradually become broader and flatter with increasing grain size. The behavior of the larger grains is consistent with observations on MD grains [10]. This change reflects the differences between PSD (grains containing only a few less mobile walls) and MD (grains containing many mobile walls). In addition all the FORC
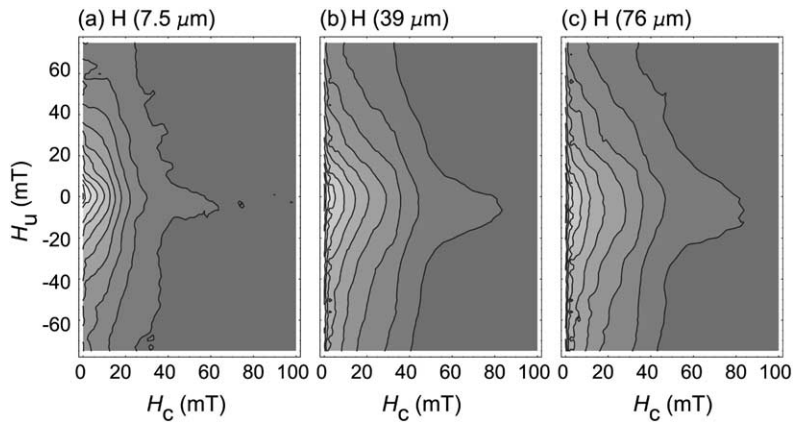
Fig. 4. Room-temperature FORC diagrams (SF = 5) for the three hydrothermally grown magnetite samples. Same scaling as Fig. 3.

distributions display strong asymmetry, which in Preisach diagrams is normally associated with the asymmetry of the interaction field during measurement [12,26].

According to Preisach–Néel SD theory, the H_U parameter is related to magnetostatic grain interactions. The theory for MD grains is less well developed, but it is clear that a system of domain walls will undergo a series of Barkhausen jumps in both increasing and decreasing fields, with an increment of magnetization at each jump. The hysteresis loop of one MD grain will resemble a linked sequence of SD loops and will generate a number of different points on a FORC distribution [26]. Domain walls in a particular grain are

best treated as a magnetostatically coupled system [27]. Thus magnetostatic interaction among domains within a grain does not shift the overall hysteresis loop, but it does result in a distribution of points in the H_U direction [10]. Importantly the interaction between domain walls, although different from interactions between SD grains, is also proportional to M_S.

6. High-temperature FORC diagrams of PSD samples

FORC diagrams were measured for the four Wright samples at either nine or 10 set temperatures up to the Curie temperature (Figs. 6 and 7). For all samples, the FORC distributions contract with increasing temperature, and the FORC distribution in the H_C direction shifts towards the H_U axis (Figs. 6–8). In particular the contours which are closed at room-temperature in samples W(0.3 μm) and W(1.7 μm) move toward the H_U axis before finally joining the axis (Figs. 6 and 8). The shape of the FORC distributions changes with temperature. The FORC distribution of the smaller samples becomes more MD-like at high temperatures. On approaching the Curie temperature it was difficult to obtain accurate FORC diagrams, because the magnetic signature of the samples became weak.

The hysteresis parameters H_C, M_{RS} and M_S were directly obtained from the FORC measure-
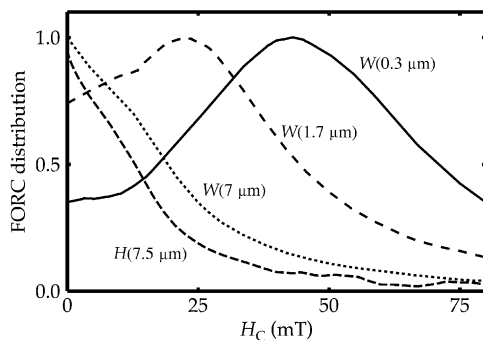

Fig. 5. Representative cross-sections along the H_C axis ($H_U = 0$) of the room-temperature FORC distributions shown in Figs. 3 and 4. According to the Preisach–Néel model this is the coercivity distribution. The H(7.5 μm) curve drops off quickly near $H_C = 0$.
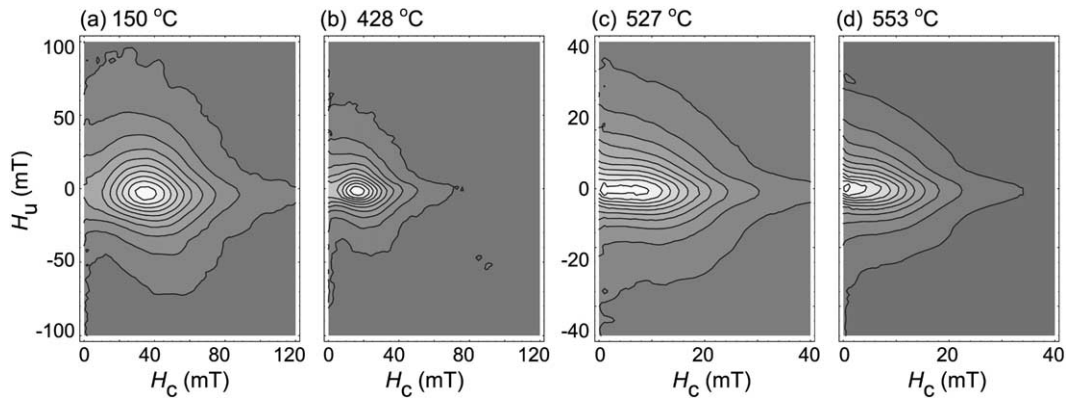
Fig. 6. FORC diagrams (SF = 2) at four elevated temperatures for sample W(0.3 µm). The scaling for parts a and b is different from that for c and d.

ments. It must be realized that determining the hysteresis parameters from FORC measurements may give slightly different values to those determined from standard hysteresis measurements because of differences in field history [12]. H_C and M_{RS}/M_S are plotted as a function of temperature in Fig. 9. On approaching the Curie temperature, H_C goes almost to zero. H_C displays similar high-temperature behavior to that reported previously [24,28]. The rate of decrease is almost constant except at very high temperatures, suggesting thermofluctuation effects are not significant at most temperatures [28]. The reduced saturation remanence similarly decreases with temperature (Fig. 9b). For sample W(0.3 µm), M_{RS}/M_S displays a

sharper decrease at high temperatures than the other three Wright samples. The most likely cause of this is chemical alteration during heating. Mössbauer spectroscopy suggests that W(0.3 µm) was initially the least stoichiometric making it the most likely to be affected by some sort of alteration on heating, i.e. inversion or reduction.

Representative transverse FORC distribution profiles in the H_U direction (nominally interaction-field spectra) are shown for sample W(1.7 µm) in Fig. 10. To ascertain how the interaction field H_U is related to the spontaneous magnetization, we consider H_i which is defined here as the full width of the distribution at half the maximum height (FWHM). Normalized H_i, i.e. $H_i(T)/$
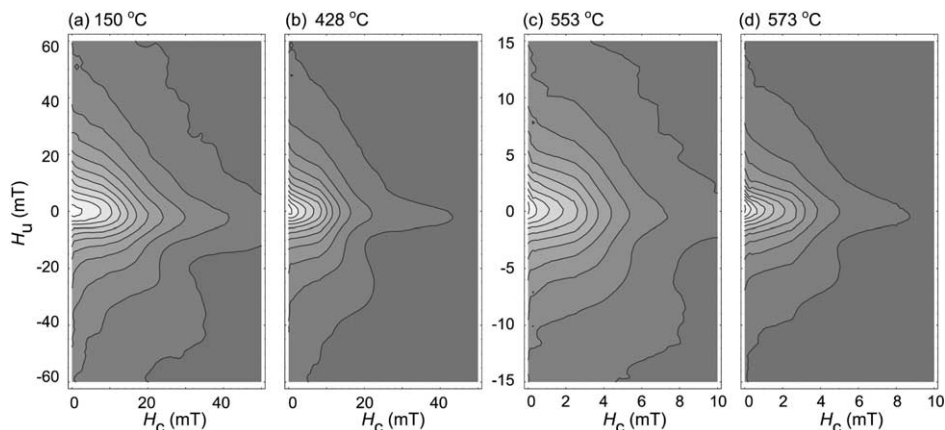

Fig. 7. FORC diagrams (SF = 3) at four elevated temperatures for sample W(7 µm). The scaling for parts a and b is different from that for c and d.
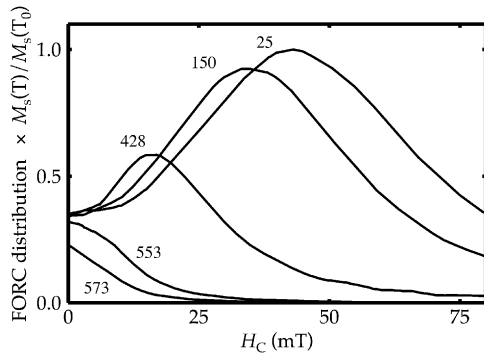
Fig. 8. Cross-sections along the H_c axis ($H_u = 0$) for the FORC distributions measured as a function of temperature for sample W(0.3 μm) (Fig. 6). The temperature for each curve is given in Celsius. The FORC distribution is multiplied by the reduced magnetization, i.e. $M_S(T)/M_S(T_0)$, where $T_0 = 25°C$.
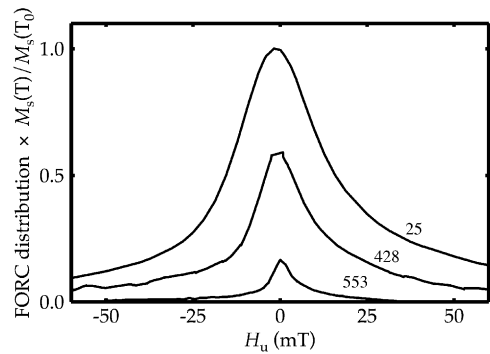

Fig. 10. Cross-sections taken in the H_U direction through the maximum of the FORC distributions measured for sample W(1.7 μm) at various temperatures. The normalized FORC distribution is multiplied by the reduced magnetization. The temperature for each curve is given in Celsius.

$H_i(25°C)$ is plotted versus $M_S(T)/M_S(25°C)$ for all four Wright samples (Fig. 11). Generally, there is a linear relationship between normalized H_i and M_S, in agreement with Néel's interpretation of Preisach theory. W(7 μm) displays strongly linear

behavior, W(1.7 μm) appears to be rather noisy, whilst both W(0.3 μm) and W(11 μm) show similar behavior which is not quite linear. Dunlop et al. [19] made similar comparisons of $H_i(T)$ and $M_S(T)$ for their Preisach diagrams. They did not find a linear relationship; instead $H_i(T)$ was more closely related to $H_C(T)$. The relationship between $H_i(T)$ and $H_C(T)$ was tested in this study, but it was not found to be linear. It is suggested that the general trend is linear and that H_U reflects the level of magnetostatic interactions.
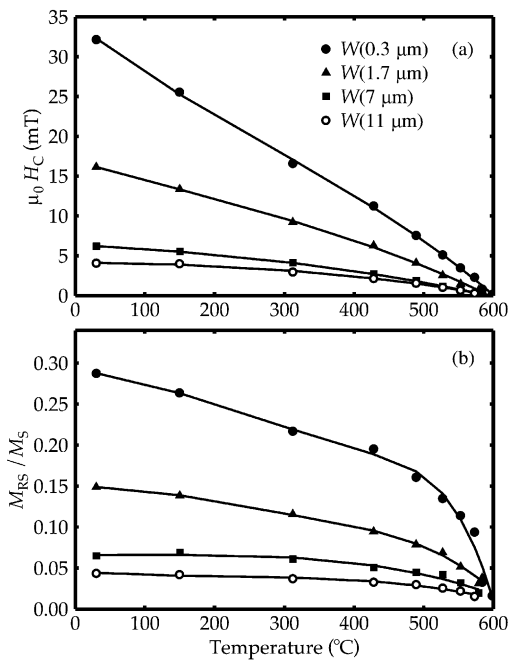

Fig. 9. As a function of temperature, (a) the coercive force and (b) the reduced remanence (M_{RS}/M_S) for all four Wright samples.

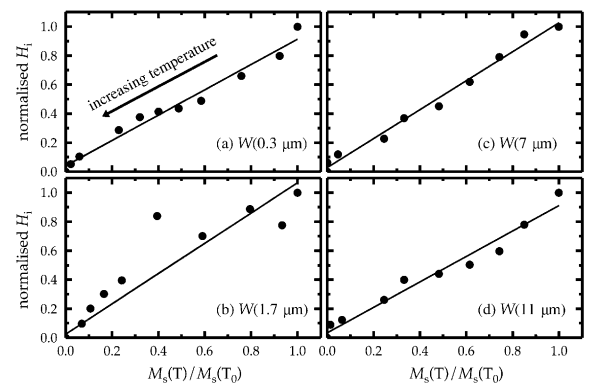
Fig. 11. Normalized H_i versus the reduced magnetization at different temperatures for samples (a) W(0.3 μm), (b) W(1.7 μm), (c) W(7 μm) and (d) W(11 μm). Linear trends have been fitted to the data. H_i is the FWHM value from cross-sections like those depicted in Fig. 10.
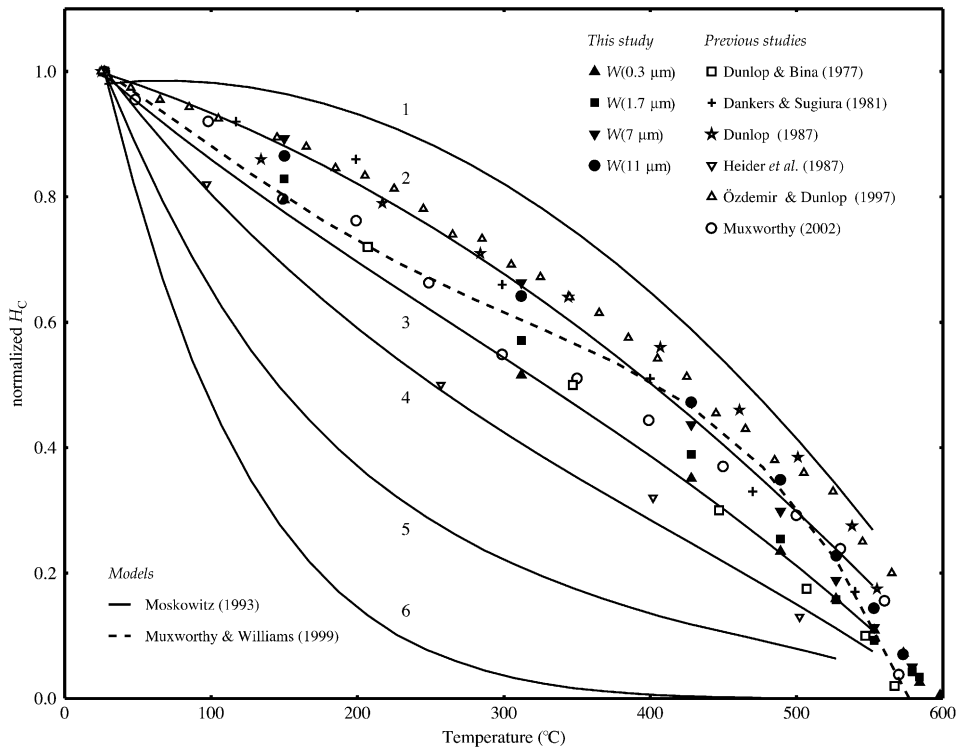
Fig. 12. Normalized coercive force versus temperature for the data plotted in Fig. 9a, compared with previously published experimental data and theoretical curves. The samples of Muxworthy [22], Heider et al. [24], Dunlop and Bina [28] and Dunlop [36] were grown synthetic magnetites with mean grain sizes of 7.5 μm (sample H(7.5 μm) in this paper), 12 μm, 1–5 μm and 0.22 μm, respectively. The 10–15 μm sample of Dankers and Sugiura [33] is shown. It was produced by annealing a crushed sample. The sample of Özdemir and Dunlop [37] was a 4 mm single crystal. The theoretical curves of Moskowitz [34] were determined using a one-dimensional pinning model and are for a 10 μm grain with six different pinning regimes; (1) positive dislocation dipole, $d/w_0 = 1$, (2) single dislocation, positive dislocation dipole $d/w_0 = 0.1$, or positive dislocation dipole bounding a stacking fault $d/w_0 = 0.1$, (3) negative dislocation dipole, $d/w_0 = 1$, (4) negative dislocation dipole, $d/w_0 = 0.1$, (5) planar defects with exchange pinning $d/w_0 = 0.1$, and (6) for planar defects with anisotropy pinning $d/w_0 = 0.1$, where the ratio d/w_0 is the reduced defect width. This dimensionless parameter sets the size of the defect and remains constant with temperature. Muxworthy and Williams [35] used a three-dimensional stress-free micromagnetic model to determine H_C for a 0.3 μm cubic grain.

To check for chemical alteration during FORC diagram measurement at high temperatures, repeat room-temperature measurements were made. In all of the samples there was evidence for some degree of alteration. For W(0.3 μm), which displayed the most alteration, after heating $\mu_0 H_C$ decreased to 25.7 mT and M_S after heating was 72% of the initial M_S. W(1.7 μm) displayed the second highest degree of alteration; $\mu_0 H_C$ after heating increased slightly to 17.2 mT and after heating M_S was 88% of the initial M_S.

7. Discussion

There is no rigorous theory for interpreting FORC diagrams for PSD and MD grains. Attempts have been made at modeling MD behavior using a one-dimensional domain wall system [10]. However, this model does not include domain wall nucleation or magnetostatic domain interactions, both of which are important during hysteresis especially in small MD grains [29,30]. The interpretation of the results in this paper is therefore based on general principles.

The room-temperature FORC measurements on the Wright magnetite samples show that there is a gradual change in the FORC distribution from SD-like (Fig. 3a,b) to MD-like (Fig. 3c,d). Samples with mean grain sizes between 1.7 μm and 7 μm need to be measured to quantify the grain size where the closed-contour structure disappears. The disappearance of the closed-contour structure could also be an indicator of the PSD-MD grain-size transition. Samples W(7 μm) (Fig. 3c) and H(7.5 μm) (Fig. 4a) have similar grain-size distributions, yet their FORC diagrams are markedly different. Sample H(7.5 μm)'s FORC diagram displays a smaller peak at the origin and is more spread out along the H_U axis, i.e. it is more MD-like. As the samples were prepared for FORC measurement using the same technique, the only possible causes for the differences are different dislocation densities and/or differences in stoichiometry.

Roberts et al. ([1], Fig. 10) illustrated a similar progression from more SD-like to more MD-like FORC distributions for sediment samples whose representative points on a Day plot had a parallel progression from SD-like to MD-like along the PSD trend. The sediments had potentially broad grain-size distributions, conceivably so broad as to include truly SD and MD end-members, and so it was uncertain whether their FORC diagrams were characteristic of single PSD sizes or blended the properties of a wide size distribution. Our results are unambiguous. Each of our samples contains grains of a distinct size, and the FORC distributions shown in Figs. 3 and 4 therefore characterize individual parts of the PSD and MD size spectrum. The combination of SD-like and MD-like features is thus a true PSD characteristic, implying contributions from both SD-like and MD-like magnetic moments in grains of a particular size, the proportions varying with grain size.

On heating the Wright samples to near the Curie temperature (Figs. 6 and 7), the FORC distributions contract toward the origin, but do not change significantly in shape or appearance until ∼500°C. If the contraction is primarily related to the decrease in M_S and H_C, then this implies that the dominant domain structure does not change

significantly with temperature. This is observed especially for the larger grains. The smaller grains with closed contours at lower temperatures become more MD-like on heating above 500°C, with the disappearance of the closed-contour structure. There are two possible causes of this change in FORC distribution. The domain structure may become more MD-like or, alternatively, the domain structure may become truly SD and then increasingly superparamagnetic, i.e. the change in FORC distribution is a SD thermal relaxation effect [9]. The first explanation appears to be more likely because recent high-resolution micromagnetic calculations [31] suggest that the SD–PSD transition size increases with temperature but it is still significantly below 0.3 μm at 565°C. This observed change in dominant domain structure may represent a possible mechanism for domain reorganization on cooling, essential for kinematic thermoremanence acquisition models [32].

According to Néel's interpretation of Preisach diagrams, $H_U \propto M_S$. If it is provisionally assumed that FORC distributions can be interpreted using Preisach theory, this relationship was found to be true at a variety of temperatures. In contrast, Dunlop et al. [19] found using Preisach diagrams for SD and small PSD samples that $H_U \propto H_C$. Initially this seems surprising, but there are certain differences in experimental method which must be considered. First, the method of experimentation was different; in this study $\rho(H_a, H_b)$ was found by measuring FORCs, whereas, Dunlop et al. [19] determined $\rho(H_a, H_b)$ from remanence measurements. Secondly, there was a large difference in the resolution used in determining $\rho(H_a, H_b)$; Dunlop et al. [19] used only 144 points to determine their distribution, whereas in this study ∼80 000 points were used.

In addition, it is also necessary to briefly consider the Preisach–Néel model. For MD grains the theory for either FORC or Preisach diagrams is not well developed. Even in a simple MD model, the interactions come from both other grains and from other magnetic domains within the grain under consideration (i.e. internal demagnetizing field). However, the MD Preisach model is more complicated than this and arguments have

been made that H_U should depend on both the microcoercive force distribution and the magnetostatic interaction energy [12,26], although this has not been rigorously tested. Assuming this to be true, if H_U is controlled by both H_C and M_S, then depending on the relative degree of interaction, the effect may be dominated by either H_C or M_S.

In this study, to try to produce strong signals at high temperatures near the Curie temperature, high concentrations of magnetite powder were mixed with the cement powder, typically on the order of 10–20% by volume. SD and PSD grains mixed in these concentrations are known to show different magnetic behavior to dispersed samples [33]. Dunlop et al. [19] used typical concentrations of only 1% by volume.

Another potentially important difference between Dunlop et al.'s samples and ours is the microcoercive force distribution and the resultant strength of domain-wall pinning (W. Williams, personal communication, 2002). Highly stressed magnetite grains like ours will tend to have their domain walls strongly pinned at the same dislocations at all temperatures. Thus the change in magnetostatic interaction due to changing M_s during heating will be the major effect and the FORC distribution in the H_U direction will contract in proportion to M_s. Low-stress hydrothermal magnetites like those used by Dunlop et al. [19] contain fewer and weaker pinning sites. During heating, the walls have more freedom of movement, jumping from one pin to another as dictated by $H_C(T)$. In this situation, the FORC and Preisach distributions in the H_U direction are likely to contract more as $H_C(T)$ than as $M_S(T)$.

All the room-temperature FORC diagrams are asymmetrical (Figs. 3 and 4), although the asymmetry decreases with temperature (Figs. 6 and 7). The origin of the asymmetry in MD grains has not been discussed in previous FORC papers. In Preisach theory, the distribution is constrained to be symmetrical. However, experimental Preisach distributions are often found to be asymmetrical [15]. Much work has been done to try to understand the asymmetry of the Preisach distribution. The primary approach has been the 'moving'

Preisach model mentioned in the introduction, which accommodates changes in the interaction field by a mean-field approach. The classical Preisach theory assumes a constant local interaction field independent of $M(H)$. In the moving model, the effective field H_{eff} is the sum of the applied field plus an interaction field proportional to the overall magnetization $M(H)$ in the applied field H:

$$H_{eff} = H + \gamma M(H) \tag{2}$$

The effectiveness of the moving Preisach model is best illustrated by considering the work of Hejda and Zelinka [15], who measured $\rho(H_a, H_b)$ using FORCs in an approach identical to that described by Roberts et al. [1], the only difference being their interpretation of the data. Hejda and Zelinka [15] considered both a classical Preisach model and a moving Preisach model. The moving Preisach model was able to account for most of the asymmetry seen in the classical Preisach model interpretation. Similarly Pike et al. [8,9] showed theoretically using a moving-Preisach-type model for SD particles that both magnetostatic interactions and thermal relaxation effects can cause asymmetry in FORC distributions. The fact that thermal relaxation effects would be expected to increase with temperature, while the asymmetry was observed to decrease (Figs. 6 and 7), suggests that the asymmetry in Preisach/FORC diagrams is directly or partially related to non-local magnetostatic interaction fields. The persistence of some asymmetry at high temperatures might be related to a non-interaction effect.

Measurements on natural rock samples containing magnetite and hematite have found that the Preisach/FORC distributions are often asymmetrical, indicating that interactions are important in geological samples, e.g. [1,9,15]. Fabian and von Dobeneck [26] suggested that for natural samples with low concentrations of magnetic minerals the classical Preisach model can be used. This may be suitable for samples containing SD or small PSD grains where interactions are due to other grains. However, where interaction effects are due primarily to domain interactions or internal demagnetizing fields, then this assumption

fails. It has been found that individual MD grains produce asymmetric FORC distributions [10].

8. Coercive force at high temperatures

Even though the understanding of hysteresis behavior of magnetite as a function of temperature is important for MD rock magnetic theories, few measurements have been reported for well-characterized stoichiometric magnetite.

The normalized coercive force as a function of temperature for samples W(0.3 μm)–W(11 μm) is compared in Fig. 12 with the one-dimensional pinning model of Moskowitz [34] and the three-dimensional micromagnetic hysteresis model of Muxworthy and Williams [35]. Moskowitz [34] examined the effect of various dislocation structures on coercive force as a function of temperature. Muxworthy and Williams [35] determined H_C for a dislocation-free 0.3 μm grain. Also depicted in Fig. 12 are experimental results of Muxworthy [22], Heider et al. [24], Dunlop and Bina [28], Dankers and Sugiura [33], Dunlop [36] and Özdemir and Dunlop [37]. The model results of Moskowitz [34] are for a 10 μm grain, implying that the model should only be directly compared with the results for W(7 μm) and W(11 μm). Moskowitz [34] showed that the microcoercive force is grain size dependent.

There is a consistent grain-size-dependent behavior for normalized H_C versus temperature (Fig. 12). Data for W(0.3 μm) falls near Moskowitz's model 3 curve, while W(1.7 μm) lies slightly above this curve. Both W(7 μm) and W(11 μm) plot near the model 2 curve. At lower temperatures, normalized H_C values for W(7 μm) are higher than those of W(11 μm), but at higher temperatures W(11 μm) has higher normalized H_C. Comparing the experimental results of this paper with those of six other studies, W(0.3 μm) and W(1.7 μm) display similar behavior to the grown sample of Dunlop and Bina [28]. Sample W(7 μm) displays behavior close to that of the annealed crushed samples of Dankers and Sugiura [33]. W(11 μm) shows similar but less pronounced behavior to that of the hydrothermal magnetite sample of Muxworthy [22], in that at higher tem-

peratures (> 400°C) the normalized H_C decreases less rapidly with temperature in agreement with the model results of Muxworthy and Williams [35] for a 0.3 μm grain. Why sample W(0.3 μm) does not display this behavior is unclear. On comparison with the model results of Moskowitz [34], the dominant pinning mechanism apparently changes with grain size. W(0.3 μm) and W(1.7 μm) are consistent with a type 3 model, W(7 μm) with a type 2 model and for W(11 μm) the dominant pinning mechanism changes with temperature, i.e. a 'combination' model [34] seems more appropriate. The 0.22 μm sample of Dunlop [36] and the 4 mm sample of Özdemir and Dunlop [37] display remarkably similar behavior, initially following the model 2 line, then switching to the model 1 curve at higher temperatures. The samples in this study have normalized $H_C(T)$ less than these two samples.

9. Conclusions

FORC diagrams have been measured as a function of temperature for a suite of sized PSD magnetite samples, and at room temperature for a set of hydrothermally grown PSD and MD magnetite samples. These measurements improve our basic understanding of this potentially important new technique, helping us to assess the contribution of interactions and the origin of the asymmetry, as well as classifying for the first time the behavior of PSD grains.

FORC diagrams gradually evolve from SD-like to MD-like through the PSD grain-size range. Small PSD grains have FORC diagrams with a distinctive closed peak structure. The FORC distributions of larger MD grains lie closer to and spread out along the H_U axis. The disappearance of the closed peak structure between samples W(1.7 μm) and W(7 μm) may indicate a boundary between PSD and MD behavior. The fact that each of our samples contains grains of a discrete size leaves no doubt that these FORC distributions are individually characteristic of PSD or MD behavior. They do not blend the properties of a broad size distribution. The evolution of the PSD diagrams from SD-like to MD-like testifies

to the changing proportions of SD-like and MD-like magnetic moments in PSD grains of different sizes.

On heating, the PSD FORC distributions contract without changing shape until $\sim 500°C$. Above this temperature, the FORC diagrams become more MD-like, with the closed-contour structures disappearing. The interaction field was temperature dependent in proportion to $M_S(T)$, in accordance with Néel's [14] interpretation of the Preisach diagram. Dunlop et al. [19] found $H_U(T) \propto H_C(T)$. It is suggested the difference between the two studies is due to different magnetite concentrations and/or differences in internal stress. In this study, the concentrations were approximately 10 times higher than those of Dunlop et al. [19].

The FORC diagrams were asymmetrical at room temperature, gradually becoming more symmetric with temperature. The decrease in asymmetry with heating suggests that its origin lies in magnetostatic interactions ($\propto M_S(T)$). This idea is supported by the direct comparison of classical and moving-model Preisach diagrams made by Hejda and Zelinka [15].

The temperature dependence of normalized coercive force varied with grain size. Samples W(0.3 μm)–W(7 μm) displayed similar smooth, nearly linear temperature dependences, with normalized H_C for W(0.3 μm) < W(1.7 μm) < W(7 μm). The trend for W(11 μm) was similar to the experimental results of Muxworthy [22] and model results of Muxworthy and Williams [35], i.e. normalized H_C did not decrease smoothly across the entire temperature range. Such behavior of H_C is potentially the origin of the demagnetization of partial thermoremanence on cooling [32].

Acknowledgements

References

[1] A.P. Roberts, C.R. Pike, K.L. Verosub, FORC diagrams: A new tool for characterizing the magnetic properties of natural samples, J. Geophys. Res. 105 (2000) 28461–28475.

[2] W. Williams, T.M. Wright, High-resolution micromagnetic models of fine grains of magnetite, J. Geophys. Res. 103 (1998) 30537–30550.

[3] S. Levi, The effect of magnetite particle size on paleointensity determinations of the geomagnetic field, Phys. Earth Planet. Inter. 13 (1977) 245–259.

[4] S.P. Lund, M. Schwartz, Environmental factors affecting geomagnetic field palaeointensity estimates from sediments, in: B.A. Maher, R. Thompson (Eds.), Quaternary Climates, Environments and Magnetism, Cambridge University Press, Cambridge, 1999, pp. 323–351.

[5] R. Day, M.D. Fuller, V.A. Schmidt, Hysteresis properties of titanomagnetites: Grain size and composition dependence, Phys. Earth Planet. Inter. 13 (1977) 260–267.

[6] D.J. Dunlop, Theory and application of the Day plot (M_{rs}/M_s versus H_{cr}/H_c) 1. Theoretical curves and tests using titanomagnetite data, J. Geophys. Res. 107 (2002) 10.1029/2001JB00486.

[7] D.J. Dunlop, Theory and application of the Day plot (M_{rs}/M_s versus H_{cr}/H_c) 2. Application to data for rocks, sediments, and soils, J. Geophys. Res. 107 (2002) 10.1029/2001JB00487.

[8] C.R. Pike, A.P. Roberts, K.L. Verosub, Characterizing interactions in fine magnetic particle systems using first order reversal curves, J. Appl. Phys. 85 (1999) 6660–6667.

[9] C.R. Pike, A.P. Roberts, K.L. Verosub, FORC diagrams and thermal relaxation effects in magnetic particles, Geophys. J. Int. 145 (2001a) 721–730.

[10] C.R. Pike, A.P. Roberts, M.J. Dekkers, K.L. Verosub, An investigation of multi-domain hysteresis mechanisms using FORC diagrams, Phys. Earth Planet. Inter. 126 (2001b) 11–25.

[11] I.D. Mayergoyz, Mathematical models of hysteresis, IEEE Trans. Magn. 22 (1986) 603–608.

[12] G. Bertotti, Hysteresis in Magnetism, Academic Press, London, 1998, 558 pp.

[13] F. Preisach, Über die magnetische Nachwirkung, Z. Phys. 94 (1935) 277–302.

[14] L. Néel, Remarques sur la théorie des propriétés magnétiques des substances dures, Appl. Sci. Res. B4 (1954) 13–24.

[15] P. Hejda, T. Zelinka, Modeling of hysteresis processes in

magnetic rock samples using the Preisach diagram, Phys. Earth Planet. Inter. 63 (1990) 32–40.

[16] D.J. Dunlop, G.F. West, An experimental evaluation of single domain theories, Rev. Geophys. 7 (1969) 709–757.

[17] V.A. Ivanov, I.A. Khaburzaniya, L.Ye. Sholpo, Use of Preisach diagram for diagnosis of single- and multi-domain grains in rock samples, Izv. Earth Phys. 17 (1981) 36–43.

[18] V.A. Ivanov, L.Ye. Sholpo, Quantitative criteria for single- and multi-domain states in ferromagnetic minerals in rocks, Izv. Earth Phys. 18 (1982) 612–616.

[19] D.J. Dunlop, M.F. Westcott-Lewis, M.E. Bailey, Preisach diagrams and anhysteresis: do they measure interactions?, Phys. Earth Planet. Inter. 65 (1990) 62–77.

[20] D.J. Dunlop, Ö. Özdemir, Rock Magnetism: Fundamentals and Frontiers, Cambridge University Press, New York, 1997, 573 pp.

[21] F. Heider, L.T. Bryndzia, Hydrothermal growth of magnetite crystals (1 μm to 1 mm), J. Cryst. Growth 84 (1987) 50–56.

[22] A.R. Muxworthy, E. McClelland, The causes of low-temperature demagnetization of remanence in multidomain magnetite, Geophys. J. Int. 140 (2000) 132–146.

[23] A.R. Muxworthy, Magnetic hysteresis and rotational hysteresis properties of hydrothermally grown multidomain magnetite, Geophys. J. Int. 149 (2002) 805–814.

[24] F. Heider, D.J. Dunlop, N. Sugiura, Magnetic properties of hydrothermally recrystallised magnetite crystals, Science 236 (1987) 1287–1290.

[25] H. Mauritsch, M. Becke, V. Kropácek, T. Zelinka, P. Hejda, Comparison of the hysteresis characteristics of synthetic samples with different magnetite and haematite contents, Phys. Earth Planet. Inter. 46 (1987) 93–99.

[26] K. Fabian, T. von Dobeneck, Isothermal magnetization of samples with stable Preisach functions: a survey of hysteresis, remanence, and rock magnetic parameters, J. Geophys. Res. 102 (1997) 17659–17677.

[27] T. Moon, R.T. Merrill, Magnetic screening in multidomain material, J. Geomagn. Geolectr. 38 (1986) 883–894.

[28] D.J. Dunlop, M.-M. Bina, The coercive force spectrum of magnetite at high temperatures: evidence for thermal activation below the blocking temperature, Geophys J. R. Astron. Soc. 51 (1977) 121–147.

[29] D. Virdee, The influence of magnetostatic interactions on the magnetic properties of magnetite, Ph.D. thesis, University of Edinburgh, 1999.

[30] A.J. Newell, R.T. Merrill, Nucleation and stability of ferromagnetic states, J. Geophys. Res. 105 (2000) 19377–19392.

[31] A.R. Muxworthy, C. Carvallo, D.J. Dunlop, W. Williams, High-resolution micromagnetic models examining magnetic stability of magnetite at elevated temperatures, J. Geophys. Res., submitted.

[32] E. McClelland, N. Sugiura, A kinematic model of TRM acquisition in multidomain magnetite, Phys. Earth Planet. Inter. 46 (1987) 9–23.

[33] P. Dankers, N. Sugiura, The effects of annealing and concentration on the hysteresis properties of magnetite around the PSD-MD transition, Earth Planet. Sci. Lett. 56 (1981) 422–428.

[34] B.M. Moskowitz, Micromagnetic study of the influence of crystal defects on coercivity in magnetite, J. Geophys. Res. 98 (1993) 18011–18026.

[35] A.R. Muxworthy, W. Williams, Micromagnetic calculation of coercive force as a function of temperature in pseudo-single domain magnetite, Geophys. Res. Lett. 26 (1999) 1065–1068.

[36] D.J. Dunlop, Temperature dependence of hysteresis in 0.04–0.22 μm magnetites and implications for domain structure, Phys. Earth Planet. Inter. 46 (1987) 100–119.

[37] Ö. Özdemir, D.J. Dunlop, Effect of crystal defects and internal stress on the domain structure and magnetic properties of magnetite, J. Geophys. Res. 102 (1997) 20211–20224.